Gravity Wave Generation by a Three-Dimensional Thermal Forcing

JADWIGA H. BERES

National Center for Atmospheric Research, Boulder, Colorado

(Manuscript received 25 August 2003, in final form 10 February 2004)

ABSTRACT

Thermal forcing is one of the mechanisms of wave generation in convection. Although it does not account for all the wave generation mechanisms, thermal forcing is a good proxy for estimating the gravity wave spectrum forced by convection. This work presents a linear theory of gravity wave generation by a three-dimensional thermal forcing assuming constant mean wind conditions in the forcing region. Relationships are derived linking the amplitude and spectral characteristics of the generated gravity waves to the properties of the thermal forcing. It is shown that the three-dimensional problem can be viewed as a multiple two-dimensional problem by means of a squire transformation and that the gravity wave properties in a given azimuthal direction depend on the projection of the heating and environmental mean wind in that direction. Shown in detail is the sensitivity of the gravity wave characteristics in three dimensions to varying heating parameters, and it is concluded that the knowledge of both horizontal and vertical scales of the heating (at least statistical), and of the environmental wind distribution, is necessary to properly parameterize convectively generated gravity waves in GCMs.

1. Introduction

Parameterization of gravity wave drag force (GWD) is critical to the proper representation of the circulations of the middle and upper atmosphere in general circulation models (GCMs; e.g., Lindzen 1981; Boville 1995). Parameterized GWD is proportional to the vertical divergence of momentum flux carried by the spectrum of upward-propagating gravity waves specified in the model. Proper representation of this quantity is dependent on the specification of the gravity wave phase speeds, horizontal wavelengths, and amplitudes above the source regions (e.g., Fritts and Alexander 2003; Kim et al. 2003). An adequate specification of these quantities is possible only once wave generation by its sources have been understood.

Convection is a major source of upward-propagating gravity waves (Alexander and Vincent 2000; Dunkerton 1997). Gravity wave generation mechanisms in convection have been a topic of many numerical modeling studies (Clark et al. 1986; Fovell et al. 1992; Alexander et al. 1995; Piani and Durran 2001). It is now widely accepted that high-frequency convectively generated gravity waves are primarily forced by the latent heating and nonlinear advection terms within the convective region (Song et al. 2003; Beres et al. 2002, 2004; Lane et al. 2001). At this point, it is unclear how the different forcing mechanisms interact with one another in convection and how to reliably represent and parameterize gravity wave forcing by these two mechanisms in different convective environments. However, several of the studies involving numerical simulation of convection have noted a strong connection between gravity wave characteristics and the properties of the latent heating. For example, Beres et al. (2002) noted that convectively generated gravity waves in the stratosphere have a dominant vertical wavelength approximately equal to the depth of tropospheric latent heating. In a study by Pandya and Alexander (1999), the authors used the spatial and temporal dependence of latent heating from a squall line simulation as forcing to a linear model. They found that the spectral properties of the linearly forced gravity waves, such as horizontal and vertical wavelengths, frequencies, and phase speeds, were the same as those of gravity waves in the fully nonlinear model. The wave amplitudes in the linear model forced by heating only, however, were higher than the amplitudes of waves in the fully nonlinear model. A recent study by Song et al. (2003) showed similar findings: linear gravity waves forced by either heating or nonlinear advection terms derived from a fully nonlinear simulation had the same spectral characteristics as gravity waves in the fully nonlinear model, but their amplitudes were much higher. Song et al. (2003) also found that when a linear model was forced with both latent heating and nonlinear advection terms derived from a nonlinear simulation, the linear gravity wave spectrum was almost exactly the same as the wave spectrum in the fully nonlinear simulation. This implies that nonlinear interactions do not play a large role in determining the convectively forced

Corresponding author address: Jadwiga H. Beres, NCAR/ASP, P.O. Box 3000, Boulder, CO 80307.
E-mail: beres@ucar.edu

gravity wave spectrum. The crucial factor in understanding the convective wave source lies in the understanding of the relationship between the nonlinear advection terms and thermal forcing.

In summary, forcing linear gravity waves using latent heating allows us to accurately deduce spectral characteristics of convectively forced gravity waves; however, using this approach, the gravity wave amplitudes are likely to be overestimated. In this study we present an analysis of the linear gravity wave response to thermal forcing alone. Although we do not consider all the wave generation mechanisms, this study is still very useful since it provides crucial links between the spectral properties of the generated gravity waves and convection properties. The work presented in this paper therefore can be used as a basis for a better source spectrum representation in GCMs with the limitation that wave amplitudes are likely to be overestimated.

Beres et al. (2004) have presented an analysis of a two-dimensional spectrum of thermally forced gravity waves. Although gravity wave parameterizations often include only eastward and westward gravity wave forcing, in reality gravity waves are predominately three-dimensional and propagate in circular patterns (in the horizontal plane) away from an isolated source region (Dewan et al. 1998; Lane et al. 2001; Piani and Durran 2001; Horinouchi et al. 2002). If there is meridional wind shear in or anywhere above the forcing region, gravity waves can exert a net meridional force on the mean flow in conjunction to a zonal force and/or the zonal force exerted by the gravity waves will be altered. Therefore, in this paper we extend the analysis of thermally forced gravity waves presented in Beres et al. (2004) to three-dimensional forcings, and describe the dependence of gravity wave zonal and meridional momentum fluxes at the top of the heating region on the source region characteristics. We also show that the three-dimensional wave generation problem can be decomposed into a multiple two-dimensional problem by the means of a squire transformation (Gage and Reid 1968). This leads to a considerable simplification of the problem and shows that wave momentum flux and wave characteristics in a given azimuthal direction depend on the projection of the mean wind and heating in that direction. In this work we also explore the sensitivity of the gravity wave spectrum to the variation of heating parameters and mean wind in the heating region. We conclude that proper assumptions about both the vertical and horizontal scales of the convective heating sources must be made in order to adequately represent the source spectrum of gravity waves in general circulation models.

2. Linear analysis

In this section we first present a solution to the three-dimensional linear Boussinesq equations for gravity waves. Subsequently we derive expressions for the vertical flux of horizontal momentum carried by gravity waves at the top of the forcing region. Three-dimensional gravity waves carry zonal momentum flux, $\rho_0 \overline{u'w'}$, as well as meridional momentum flux, $\rho_0 \overline{v'w'}$. The formulation for those two quantities is derived in section 2b. In general circulation models it is sometimes more appropriate to specify wave momentum flux in different azimuthal angles instead of specifying $\rho_0 \overline{u'w'}$ and $\rho_0 \overline{v'w'}$. This formulation of momentum flux is derived in section 2c.

Note that using this method of specifying gravity wave momentum flux in a GCM, gravity waves can be launched at the top of convection instead of at a fixed source level. That is of course if the gravity wave parameterization scheme allows such a modification; otherwise, the gravity wave source spectrum derived at the top of the heating must be adjusted for critical-level filtering between the top of the convective heating and the gravity wave source level.

a. Solution to equations of motion

The three-dimensional Boussinesq equations of motions for linear gravity waves generated by a thermal forcing in the presence of constant zonal mean wind $\overline{U}$ and meridional mean wind $\overline{V}$ can be written as

$$\frac{\partial u'}{\partial t} + \overline{U}\frac{\partial u'}{\partial x} + \overline{V}\frac{\partial u'}{\partial y} + \frac{1}{\rho_0}\frac{\partial p'}{\partial x} = 0, \quad (1)$$

$$\frac{\partial v'}{\partial t} + \overline{U}\frac{\partial v'}{\partial x} + \overline{V}\frac{\partial v'}{\partial y} + \frac{1}{\rho_0}\frac{\partial p'}{\partial y} = 0, \quad (2)$$

$$\frac{\partial w'}{\partial t} + \overline{U}\frac{\partial w'}{\partial x} + \overline{V}\frac{\partial w'}{\partial y} + \frac{1}{\rho_0}\frac{\partial p'}{\partial z} - g\frac{\theta'}{\theta_0} = 0, \quad (3)$$

$$\frac{\partial u'}{\partial x} + \frac{\partial v'}{\partial y} + \frac{\partial w'}{\partial z} = 0, \quad (4)$$

$$\frac{g}{\theta_0}\left(\frac{\partial \theta'}{\partial t} + \overline{U}\frac{\partial \theta'}{\partial x} + \overline{V}\frac{\partial \theta'}{\partial y}\right) + w'N^2 = \frac{g}{\theta_0}J', \quad (5)$$

where (1), (2), and (3) are the zonal, meridional, and vertical momentum equations respectively, (4) is the continuity equation, and (5) is the thermodynamic equation. In the preceding, u', v', and w' represent the three components of perturbation velocity (zonal, meridional, and vertical), p' represents perturbation pressure, and θ' represents perturbation potential temperature; ρ_0 and θ_0 are constant basic-state values for density and potential temperature. The buoyancy frequency N is taken to be constant with height. The effects of the Coriolis force are excluded from the analysis.

The term $(g/\theta_0)J'$ in (5) represents the thermal forcing as a function of space and time. In order to solve the problem analytically, we assume that the forcing has a separable dependence in x, y, z, and t, and we express it as

$$\frac{g}{\theta_0}J' = Q_0 q_x(x) q_y(y) q_z(z) q_t(t), \quad (6)$$

where q_x and q_y represent heating-rate variations in the zonal and meridional directions, q_z represents variations

in the vertical, q_t represents temporal variations, and Q_0 is the heating-rate amplitude.

Equations (1)–(5) can be combined into a single equation describing the perturbation vertical velocity field:

$$\left(\frac{\partial}{\partial t} + \overline{U}\frac{\partial}{\partial x} + \overline{V}\frac{\partial}{\partial y}\right)^2\left(\frac{\partial^2}{\partial x^2} + \frac{\partial^2}{\partial y^2} + \frac{\partial^2}{\partial z^2}\right)w' + N^2\left(\frac{\partial^2}{\partial x^2} + \frac{\partial^2}{\partial y^2}\right)w' = \frac{g}{\theta_0}\left(\frac{\partial^2}{\partial x^2} + \frac{\partial^2}{\partial y^2}\right)J'. \quad (7)$$

Further, we assume that the forcing has a Gaussian distribution in the horizontal and a half-sine wave structure in the vertical:

$$q_x(x) = \exp\left[-\frac{(x - x_0)^2}{\sigma_x^2}\right], \quad (8)$$

$$q_y(y) = \exp\left[-\frac{(y - y_0)^2}{\sigma_y^2}\right], \quad (9)$$

$$q_z(z) = \begin{cases} \sin(\pi z/h) & \text{for } 0 \le z \le h \\ 0 & \text{for } z > h. \end{cases} \quad (10)$$

The heat source therefore has a horizontal scale of approximately $2\sigma_x$ in the zonal direction, $2\sigma_y$ in the meridional direction, and a depth of h. The horizontal distribution of the heating can be expressed in terms of the Fourier components of the forcing. For the zonal direction this expression is

$$q_x(x) = \frac{1}{\sqrt{2\pi}}\int_{-\infty}^{+\infty} Q_x(k)e^{ikx}\,dk, \quad (11)$$

where Q_x is the Fourier transform of the zonal distribution of the heating q_x:

$$Q_x(k) = \frac{1}{\sqrt{2\pi}}\int_{-\infty}^{+\infty} q_x(x)e^{-ikx}\,dx, \quad (12)$$

where k is the zonal wavenumber. An analogous expression can be derived for the Fourier transform of the meridional heating distribution, Q_y, as a function of the meridional wavenumber l.

For the horizontal heating distribution specified in (8) and (9), Q_x and Q_y take the following form:

$$Q_x(k) = \frac{\sigma_x}{\sqrt{2}}\exp\left(\frac{-k^2\sigma_x^2}{4}\right), \quad (13)$$

$$Q_y(l) = \frac{\sigma_y}{\sqrt{2}}\exp\left(\frac{-l^2\sigma_y^2}{4}\right), \quad (14)$$

with the phase shift ignored.

Similarly, the temporal distribution of the forcing, $q_t(t)$, can be represented as a linear sum of individual frequency components of the forcing:

$$q_t(t) = \frac{1}{\sqrt{2\pi}}\int_{-\infty}^{+\infty} Q_t(\nu)e^{-i\nu t}\,d\nu, \quad (15)$$

where Q_t is the Fourier transform of q_t, and values of ν represent forcing frequencies relative to the ground or stationary forcing region.

The thermal forcing can be therefore written as an integral of its spectral components in both space and time:

$$\frac{g}{\theta_0}J' = (2\pi)^{-(3/2)}q_z(z)Q_0\int_{-\infty}^{+\infty}\int_{-\infty}^{+\infty}\int_{-\infty}^{+\infty} Q_x(k)Q_y(l)Q_t(\nu)e^{i(kx+ly-\nu t)}\,dk\,dl\,d\nu. \quad (16)$$

The general solution to (7) has the form

$$w'(x, z, t) = (2\pi)^{-(3/2)}\int_{-\infty}^{+\infty}\int_{-\infty}^{+\infty}\int_{-\infty}^{+\infty} W_{kl\nu}(z)e^{i(kx+ly-\nu t)}\,dk\,dl\,d\nu, \quad (17)$$

where $W_{kl\nu}$ gives the height dependence of the vertical velocity component with zonal wavenumber k, meridional wavenumber l, and frequency ν.

The substitution of (16) and (17) into (7) gives the height dependence of each spectral component of vertical velocity:

$$\hat{\nu}^2\left[-(k^2 + l^2) + \frac{d^2}{dz^2}\right]W_{kl\nu}(z) + N^2(k^2 + l^2)W_{kl\nu}(z) = (k^2 + l^2)Q_0Q_x(k)Q_y(l)Q_t(\nu)q_z(z), \quad (18)$$

where $\hat{\nu}$ is the intrinsic frequency defined as

$$\hat{\nu} = \nu - \overline{U}k - \overline{V}l. \quad (19)$$

For $\hat{\nu} \neq 0$ (18) can be rewritten as

$$\frac{d^2W_{kl\nu}}{dz^2} + m_{kl\nu}^2W_{kl\nu} = \frac{(k^2 + l^2)}{\hat{\nu}^2}Q_0Q_x(k)Q_y(l)Q_t(\nu)q_z(z), \quad (20)$$

where $m_{kl\nu}$ is defined as

$$m_{kl\nu}^2 = (k^2 + l^2)\left(\frac{N^2}{\hat{\nu}^2} - 1\right). \quad (21)$$

Above the forcing region $m_{kl\nu}$ represents the wave vertical wavenumber.

In our subsequent analysis we use the following convention for distinguishing the direction of wave prop-

agation: we consider waves with positive frequencies ν only and let the positive and negative zonal (meridional) wavenumbers distinguish the eastward (northward)- and westward (southward)-propagating wave modes relative to the ground. In this configuration, we must choose the sign of $m_{kl\nu}$ to be negative in order to ensure upward energy propagation.

The solution to (20) in the heating region $0 \leq z \leq h$ satisfying the lower boundary condition $w = 0$ at $z = 0$ is

$$W_{kl\nu}(z) = A_{kl\nu} \sin(m_{kl\nu} z) + A'_{kl\nu} \sin(\pi z/h), \quad (22)$$

where

$$A'_{kl\nu} = \frac{(k^2 + l^2)}{\hat{\nu}^2 (m_{kl\nu}^2 - \pi^2/h^2)} Q_0 Q_x Q_y Q_t. \quad (23)$$

For $z > h$, the vertical velocity of the upward energy carrying wave mode satisfying the radiation condition as $z \to \infty$ is

$$W_{kl\nu}(z) = B_{kl\nu} e^{-i m_{kl\nu} z}. \quad (24)$$

The coefficients $A_{kl\nu}$ and $B_{kl\nu}$ in (22) and in (24) are determined by the condition that w' and $\partial w'/\partial z$ must be continuous at $z = h$. Therefore $A_{kl\nu}$ is

$$A_{kl\nu} = A'_{kl\nu} \left(\frac{\pi}{m_{kl\nu} h} \right) \exp(-i m_{kl\nu} h). \quad (25)$$

The coefficient $B_{kl\nu}$ is

$$B_{kl\nu} = A'_{kl\nu} \left(\frac{\pi}{m_{kl\nu} h} \right) \sin(m_{kl\nu} h). \quad (26)$$

For $l = 0$, the preceding solution reduces to Beres et al.'s (2004) solution for a two-dimensional forcing. The amplitude of a wave mode with given horizontal wavenumbers k and l at a given frequency ν depends on the wave intrinsic frequency, $\hat{\nu}$; hence, the effects of the mean wind within the heating region can not be ignored.

b. Zonal and meridional wave momentum fluxes

The zonal component of the wave momentum flux, $\rho_0 \overline{u'w'}$, is equal to the sum of the zonal momentum flux carried by gravity waves at each forcing frequency, $F_x(\nu)$,

$$\rho_0 \overline{u'w'} = \int_0^{+\infty} F_x(\nu)\, d\nu, \quad (27)$$

where the overbar represents a horizontal domain average.

Similarly, the momentum flux carried by gravity waves in the meridional direction, $\rho_0 \overline{v'w'}$, can be expressed as

$$\rho_0 \overline{v'w'} = \int_0^{+\infty} F_y(\nu)\, d\nu. \quad (28)$$

The momentum flux in the zonal (F_x) and meridional directions (F_y) at each forcing frequency can then be written in terms of the spectral components of the vertical and horizontal velocity at that frequency, $U_{kl\nu}$, $V_{kl\nu}$, and $W_{kl\nu}$;

$$F_x(\nu) = \frac{1}{2\pi} \frac{\rho_0}{L_x L_y \tau} \int_{-\infty}^{+\infty} \int_{-\infty}^{+\infty} U_{kl\nu} W^*_{kl\nu}\, dk\, dl, \quad (29)$$

$$F_y(\nu) = \frac{1}{2\pi} \frac{\rho_0}{L_x L_y \tau} \int_{-\infty}^{+\infty} \int_{-\infty}^{+\infty} V_{kl\nu} W^*_{kl\nu}\, dk\, dl, \quad (30)$$

where the asterisk denotes a complex conjugate, L_x and L_y represent the lengths of the domain in the zonal and meridional directions, respectively, and τ is a time interval.

Using the horizontal momentum equations (1) and (2), the continuity equation (4), and dispersion relation (21), we can rewrite the spectral horizontal velocity components in terms of the spectral vertical velocity component:

$$U_{kl\nu} = -\frac{m_{kl\nu} k}{(k^2 + l^2)} W_{kl\nu}, \quad (31)$$

$$V_{kl\nu} = -\frac{m_{kl\nu} l}{(k^2 + l^2)} W_{kl\nu}. \quad (32)$$

Substitution of (29) and (31) into (27) yields an expressions for the domain-averaged zonal momentum flux from a multifrequency thermal forcing above the forcing region:

$$\rho_0 \overline{u'w'} = \int_0^{+\infty} \int_{-\infty}^{+\infty} \int_{-\infty}^{+\infty} FU_{kl\nu}(k, l, \nu)\, dk\, dl\, d\nu, \quad (33)$$

where

$$FU_{kl\nu}(k, l, \nu) = -\frac{1}{2\pi} \frac{\rho_0}{L_x L_y \tau} \frac{m_{kl\nu} k}{(k^2 + l^2)} |B_{kl\nu}|^2. \quad (34)$$

Similarly, the substitution of (30) and (32) into (28) yields an expression for the domain-averaged meridional momentum flux:

$$\rho_0 \overline{v'w'} = \int_0^{+\infty} \int_{-\infty}^{+\infty} \int_{-\infty}^{+\infty} FV_{kl\nu}(k, l, \nu)\, dk\, dl\, d\nu, \quad (35)$$

where

$$FV_{kl\nu}(k, l, \nu) = -\frac{1}{2\pi} \frac{\rho_0}{L_x L_y \tau} \frac{m_{kl\nu} l}{(k^2 + l^2)} |B_{kl\nu}|^2. \quad (36)$$

Here, $FU_{kl\nu}$ and $FV_{kl\nu}$ yield the distribution of wave momentum flux across zonal and meridional wavenumbers and frequencies. Note that (33) and (35) hold only for nonzero intrinsic frequencies. The values $\rho_0 \overline{u'w'}$ and $\rho_0 \overline{v'w'}$ are 0 for $\hat{\nu} = 0$.

Using the preceding notation, the momentum flux magnitude, M, can be written as

$$M = [(\rho_0 \overline{u'w'})^2 + (\rho_0 \overline{v'w'})^2]^{1/2}. \quad (37)$$

c. Wave momentum flux as a function of azimuthal angle

In general circulation models it is appropriate to launch a spectrum of gravity waves in several directions at the source altitude. For this reason, using the analysis that follows, we arrive at an expression that specifies wave momentum flux at different angles from the eastward direction, ϕ ($\phi = 0$ for an eastward-propagating wave, $\phi = \pi/2$ for a northward-propagating wave, etc.). In other words, we derive at the quantity $F_\phi(\tilde{k}, \phi, \nu)$, wave momentum flux as a function of horizontal wavenumber, $\tilde{k}$, azimuthal angle, ϕ, and frequency ν. This formulation is simpler and quicker to calculate than calculating $FU_{kl\nu}(k, l, \nu)$ and $FV_{kl\nu}(k, l, \nu)$.

In order to derive at a formulation for $F_\phi(\tilde{k}, \phi, \nu)$ we apply a squire transformation (Gage and Reid 1968) to the equations of motion [(1)–(5)], which reduces the three-dimensional problem to a two-dimensional one. In order to make this transformation we let

$$\tilde{k} = (k^2 + l^2)^{1/2}, \tag{38}$$

$$\sin\phi = \frac{l}{\tilde{k}} \qquad \cos\phi = \frac{k}{\tilde{k}}, \tag{39}$$

$$\tilde{k}\tilde{u} = ku' + lv', \tag{40}$$

$$\tilde{k}\tilde{\overline{U}} = k\overline{U} + l\overline{V}, \tag{41}$$

or alternatively

$$\tilde{\overline{U}} = \overline{U}\cos\phi + \overline{V}\sin\phi, \tag{42}$$

$$\tilde{\hat{\nu}} = \nu - \tilde{k}\tilde{\overline{U}}, \tag{43}$$

$$\tilde{m}^2_{\tilde{k}\phi\nu} = \tilde{k}^2\left(\frac{N^2}{\tilde{\hat{\nu}}^2} - 1\right), \tag{44}$$

$$(\tilde{\sigma}_{xy}\tilde{k})^2 = (\sigma_x k)^2 + (\sigma_y l)^2, \tag{45}$$

$$\tilde{\sigma}^2_{xy} = (\sigma_x\cos\phi)^2 + (\sigma_y\sin\phi)^2, \tag{46}$$

$$\tilde{Q}_{xy}(\tilde{k}) = Q_x(k)Q_y(l). \tag{47}$$

Here, $\tilde{k}$ is the horizontal wavenumber in the direction of angle ϕ and $\tilde{m}_{\tilde{k}\phi\nu}$ is the corresponding vertical wavenumber. Similarly $\tilde{\overline{U}}$ represents the mean wind, and $\tilde{\sigma}_{xy}$ represents horizontal heating scale in this direction. (Note that $\tilde{m}_{\tilde{k}\phi\nu}$ and $m_{kl\nu}$, and $\tilde{\hat{\nu}}$ and $\hat{\nu}$ are equivalent to each other, however, after the transformation we are not considering k and l pairs to define the wave propagation direction; instead we use $\tilde{k}$ and ϕ).

After applying the squire transformation to the equation of motions [(1)–(5)] we can rewrite (20) as

$$\frac{d^2\tilde{W}_{\tilde{k}\phi\nu}}{dz^2} + \tilde{m}^2_{\tilde{k}\phi\nu}\tilde{W}_{\tilde{k}\phi\nu} = \frac{\tilde{k}^2}{\tilde{\hat{\nu}}^2}Q_0\tilde{Q}_{xy}(\tilde{k})Q_t(\nu)q_z(z), \tag{48}$$

where $\tilde{W}_{\tilde{k}\phi\nu}$ represents the vertical velocity amplitude of a wave mode with horizontal wavenumber $\tilde{k}$ and frequency ν.

Using this notation, the domain-averaged momentum flux magnitude, M is

$$M = \int_0^{2\pi}\int_0^{+\infty}\int_0^{+\infty} F_\phi(\tilde{k}, \phi, \nu)\, d\nu\, d\tilde{k}\, d\phi, \tag{49}$$

where F_ϕ is the momentum flux per unit angle, unit frequency, and unit wavenumber, at an angle ϕ from the eastward direction. Here, F_ϕ is

$$F_\phi = \frac{1}{2\pi^{3/2}}\frac{\rho_0}{L_{xy}\tau}\tilde{U}_{\tilde{k}\phi\omega}\tilde{W}^*_{\tilde{k}\phi\nu}, \tag{50}$$

where

$$\tilde{U}_{\tilde{k}\phi\nu}\tilde{W}^*_{\tilde{k}\phi\nu} = \left(\frac{\tilde{m}_{\tilde{k}\phi\nu}}{\tilde{k}}\right)|\tilde{B}_{\tilde{k}\phi\nu}|^2 = \left(\frac{N^2}{\tilde{\hat{\nu}}^2} - 1\right)^{1/2}|\tilde{B}_{\tilde{k}\phi\nu}|^2. \tag{51}$$

For $\phi = 0$, $\tilde{B}_{\tilde{k}\phi\nu}$ is equal to $B_{k\nu}$ in two dimensions (Beres et al. 2004):

$$\tilde{B}_{\tilde{k}\phi\nu} = \hat{A}'_{\tilde{k}\phi\nu}\left(\frac{\pi}{\tilde{m}_{\tilde{k}\phi\nu}h}\right)\sin(\tilde{m}_{\tilde{k}\phi\nu}h), \tag{52}$$

where

$$A'_{\tilde{k}\nu} = \frac{\tilde{k}^2}{\tilde{\hat{\nu}}^2(\tilde{m}^2_{\tilde{k}\nu} - \pi^2/h^2)}Q_0\tilde{Q}_{xy}Q_t. \tag{53}$$

The spectral properties of a gravity wave in a given azimuthal direction are therefore dependent on the projection of the mean wind vector in the direction of wave propagation $\tilde{\overline{U}}$, and the projection of the heating in that direction $\tilde{Q}_{xy}$. The quantity $\tilde{Q}_{xy}$ is primarily linearly dependent on the horizontal extent of the heating in the direction ϕ, $\tilde{\sigma}_{xy}$. Each azimuthal direction being considered therefore can be treated as a separate two-dimensional wave forcing problem. For $\overline{U} = \overline{V} = 0$ and $\sigma_x = \sigma_y$, $\tilde{\overline{U}}$ and $\tilde{\sigma}_{xy}$ are the same for all values of ϕ and the wave field is the same in all azimuthal directions.

3. Sensitivity of the wave spectrum to heating parameters

The equations derived in the previous section allow for the estimation of gravity wave momentum flux and their spectral properties at the top of the heating region, given that the convective region properties (depth, horizontal scales, frequency distribution, heating rate, environmental buoyancy frequency, and wind) are known. In general circulation models not all these parameters are available, therefore some assumptions need to be made. Below we examine the sensitivity of the linear gravity wave spectrum to the forcing parameters. The gravity wave characteristics that we will compare are the dominant wave phase speed, dominant horizontal wavelength, and maximum and total magnitude of momentum flux in a given direction. These quantities are most relevant to parameterizations of gravity waves in GCMs.

The previously described wave characteristics will be derived from the following two quantities: wave momentum flux per unit wavenumber and angle, $F_{\tilde{k}\phi}(\tilde{k}, \phi)$,

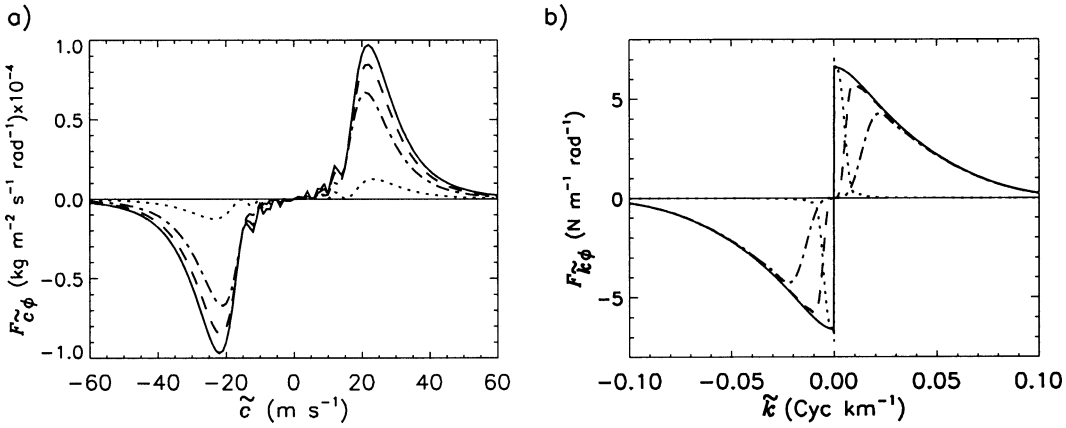

FIG. 1. Momentum flux carried by thermally forced gravity waves in each azimuthal direction for a heat source with a frequency distribution given by (55), vertical scale $h = 8$ km, and horizontal scale $\sigma_x = 3$ km. (a) The momentum flux spectrum as a function of wave phase speed, $F_{\tilde{c}\phi}$. (b) The distribution as a function of wave horizontal wavenumber, $F_{\tilde{k}\phi}$. Different line types represent different frequency integration limts in (54): for the solid line: $\nu_{\min} = 0$, $\nu_{\max} = 2\pi/10$ min; dotted line: $\nu_{\min} = 0$, $\nu_{\max} = 2\pi/100$ min; dashed line: $\nu_{\min} = 2\pi/100$ min, $\nu_{\max} = 2\pi/10$ min; dashed–dotted line: $\nu_{\min} = 2\pi/60$ min, $\nu_{\max} = 2\pi/10$ min.

and wave momentum flux per unit phase speed and angle, $F_{\tilde{c},\phi}(\tilde{c}, \phi)$. Both quantities are derived by integrating $F_{\phi}(\tilde{k}, \phi, \nu)$ over a specified range of frequencies. The range of frequencies will be described in the following subsection. Hence, $F_{\tilde{k}\phi}(\tilde{k}, \phi)$ is calculated as follows:

$$F_{\tilde{k}\phi}(\tilde{k}, \phi) = \int_{\nu_{\min}}^{\nu_{\max}} F_{\phi}(\tilde{k}, \phi, \nu)\, d\nu. \tag{54}$$

The calculation of $F_{\tilde{c}\phi}(\tilde{c}, \phi)$ from $F_{\phi}(\tilde{k}, \phi, \nu)$ requires binning together of F_{ϕ} values for the same values of $\tilde{c} = \nu/\tilde{k}$.

Holton et al. (2002) have shown that spectral characteristics of thermally forced gravity waves are dependent on the forcing frequency, depth, and horizontal scale. Since these quantities are not resolved in a GCM we need to make some assumptions about them. In the following sections we assess how the choice of forcing parameters affects the gravity wave field. We begin with examining the assumption about the forcing frequency.

a. Frequency

In realistic convection, the latent heating consists of a spectrum of frequencies. Beres et al. (2004) showed that the latent heating spectrum in a numerical squall line simulation is fairly close to a red-noise frequency distribution, and can be written as

$$Q_{\nu}(\nu) = Q_0 \times \left[\frac{1}{(1 + \nu^2 \times 100^2)}\right]. \tag{55}$$

Although the convective heating exhibits a full range of periods, ranging from several minutes to several days, gravity waves in numerical simulations are mostly observed with periods between 10 and 100 min (Alexander et al. 1995; Song et al. 2003). We show later that is mainly because small-scale convective elements, $\sigma_x \approx$ 1–10 km, force gravity waves efficiently at high frequencies (wave periods between 10 and 100 min). Longer-period gravity waves are generated more efficiently from forcing with larger horizontal scales.

Let us first consider a motionless atmosphere, $U = V = 0$, and a thermal forcing with $\sigma_x = \sigma_y = 3$ km and $h = 8$ km. For such a forcing, the gravity wave field is the same in all azimuthal directions. Let us also assume that the forcing frequencies range from $N \leq \nu \leq 0.01$ s^{-1} (10 min $\leq T \leq$ 7.25 days). For this forcing, Fig. 1 shows the distribution of wave momentum flux across phase speeds, $F_{\phi,\tilde{c}}$ (Fig. 1a), and of wave momentum flux across horizontal wavenumbers, $F_{\phi,\tilde{k}}$ (Fig. 1b), in each azimuthal direction. Different line types represent different regions of the frequency spectrum that wave momentum flux is integrated over. For this figure, and throughout the rest of this paper, we assume buoyancy frequency in the heating region of $N = 0.012$ s^{-1}, heating rate $Q_0 = 0.004$ K s^{-1}, and $L_{xy} = 1 \times 10^6$ km.

Figure 1 shows that 85% of the gravity wave momentum flux is carried by gravity waves with periods between 10 and 100 min. Although most of the latent heating is at lower frequencies, wave generation at horizontal scales of order of 1 km is not efficient for waves with periods longer than a 100 min. Sixty-five percent of the wave momentum flux is carried by waves with periods less than 60 min, which implies that it is the very high frequency waves that generate largest amounts of momentum flux from small convective elements.

Figure 1a shows that the dominant phase speed of the gravity waves generated by the considered forcing is 21 m s^{-1} independent of wave frequency. The dominant horizontal wavenumber of the generated waves, how-

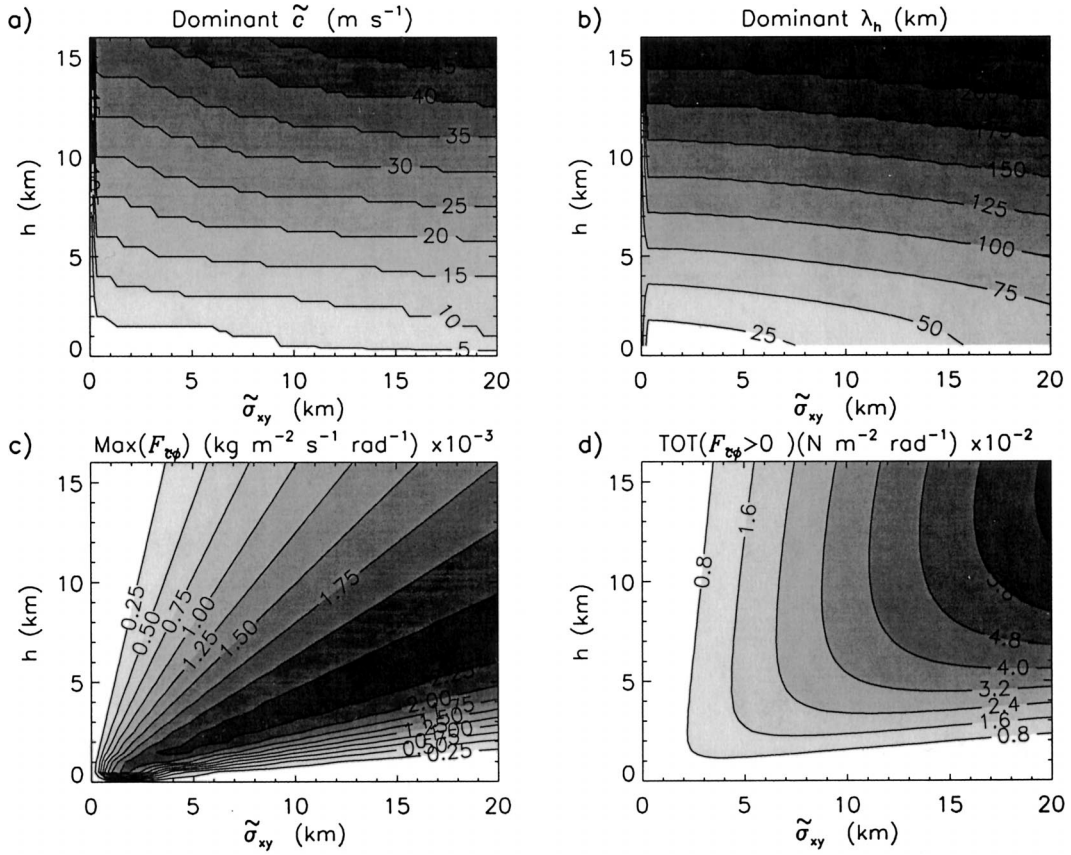

FIG. 2. Dependence of thermally forced gravity wave characteristics on heating depth and horizontal scale: (a) dominant wave phase speed, c; (b) dominant horizontal wavelength, λ_h; (c) maximum momentum flux value, max($F_{\tilde{c}\phi}$); and (d) absolute value of total momentum flux in each direction, TOT($F_{\tilde{c}\phi}$).

ever, increases as the wave frequency increases. Waves with periods between 10 and 100 min have a dominant horizontal wavelength of ~100 km [$\tilde{k} \sim 0.01$ cycles per kilometer (cpk)], waves with periods between 10 and 60 min have a dominant horizontal wavelength of 45 km ($\tilde{k} \sim 0.022$ cpk). Therefore, the assumption of wave frequencies present impacts the dominant horizontal wavelength of gravity waves. Ideally, in a GCM, one would specify the full spectrum of wave frequencies and horizontal wavenumbers, however, currently gravity wave parameterization do not allow such flexibility.

The earlier-described characteristics of high-frequency waves predicted by linear theory are consistent with the numerical studies of Piani and Durran (2001) who noted the dominant horizontal wavelengths of convectively forced gravity waves to be between 50 and 75 km. Lane et al. (2001) and Horinouchi et al. (2002) noted that the dominant horizontal wavelength of gravity waves in their simulations were between 15 and 20 km, implying that waves with periods of about 20 min were responsible for most of the wave generation. Hence, the choice of dominant wave frequencies may be dependent on convection type; however, in current GCMs some kind of assumption must be made. In the following sections we show further sensitivity studies with gravity wave momentum flux carried by waves with periods between 10 and 100 min, but we remind readers that this assumption may not always be the best one. More observational studies are needed to constrain this.

b. Heating size

The dominant wave phase speed, the dominant horizontal wavelength, the peak momentum flux value, and the total momentum flux magnitude in each azimuthal direction shown in Fig. 1 vary with the size of the thermal forcing. Figure 2 summarizes the sensitivity of these wave spectrum characteristics to the horizontal and vertical scales of the heating for waves with periods between 10 and 100 min.

The vertical scale of the heating primarily influences the dominant wave phase speed and dominant horizontal wavelength at which gravity waves are generated, as well as the width of the momentum flux phase speed spectra. Figure 2a shows that the dominant wave phase speed increases strongly with increasing heating depth.

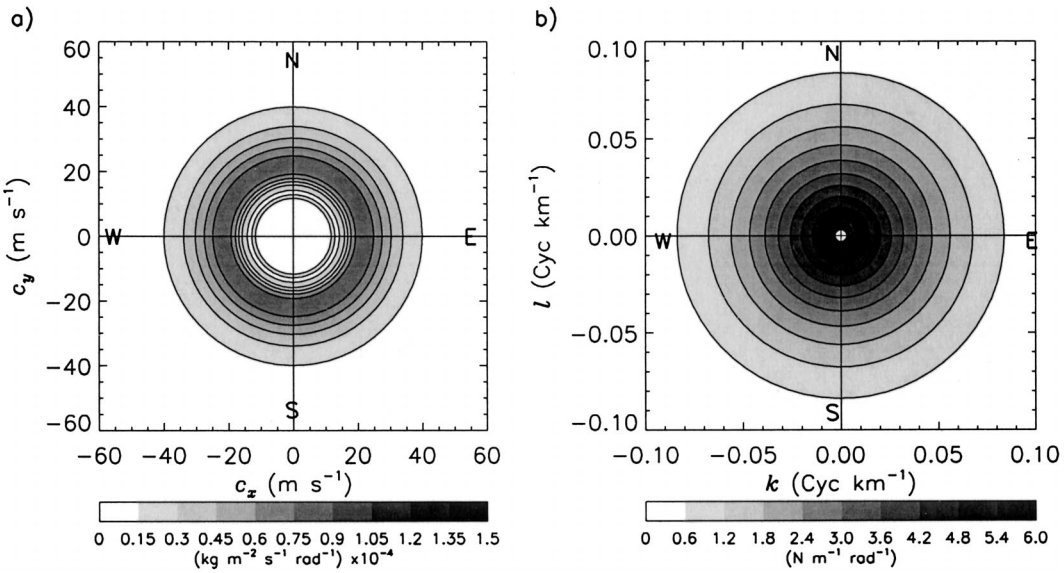

FIG. 3. Three-dimensional momentum flux spectrum of gravity waves with periods between 10 and 100 min forced by a thermal forcing with $h = 8$ km, $\sigma_x = \sigma_y = 3$ km, and frequency distribution given by (55). (a) The momentum flux spectrum as a function of wave phase speed and azimuthal angle, $F_{\tilde{c}\phi}$ [x axis shows phase speed in the x direction, c_x; y axis shows wave phase speed in the y direction, c_y; $\tilde{c} = (c_x^2 + c_y^2)^{1/2}$]. (b) Momentum flux magnitude as a function of horizontal wavenumber and azimuthal angle, $F_{\tilde{k}\phi}$ (x axis depicts the horizontal wavenumber k, and the y axis depicts the meridional wavenumber l). Bold letters E, N, W, S mark the east, north, west, and south directions corresponding to azimuthal angles 0, $\pi/2$, π, and $3\pi/2$, respectively.

The dominant wave phase speed is rather insensitive to the horizontal scale of the heating, especially for heating cells with $\sigma_x > 10$ km. The dominant horizontal wavelength of convectively generated gravity waves (Fig. 2b) also depends much more strongly on the heating depth than the horizontal scale of the heating. This might be a surprising result, however, the wave phase speed is proportional to the wave frequency and horizontal wavelength; hence, for a small range of wave frequencies, changes in horizontal wavelength will follow changes in wave phase speed. As wave phase speed is nearly independent of the horizontal scale of the heating, the dominant horizontal wavelength of gravity waves follows this relationship as well.

Figure 2c shows that the peak momentum flux amplitude carried by the dominant wave mode decreases

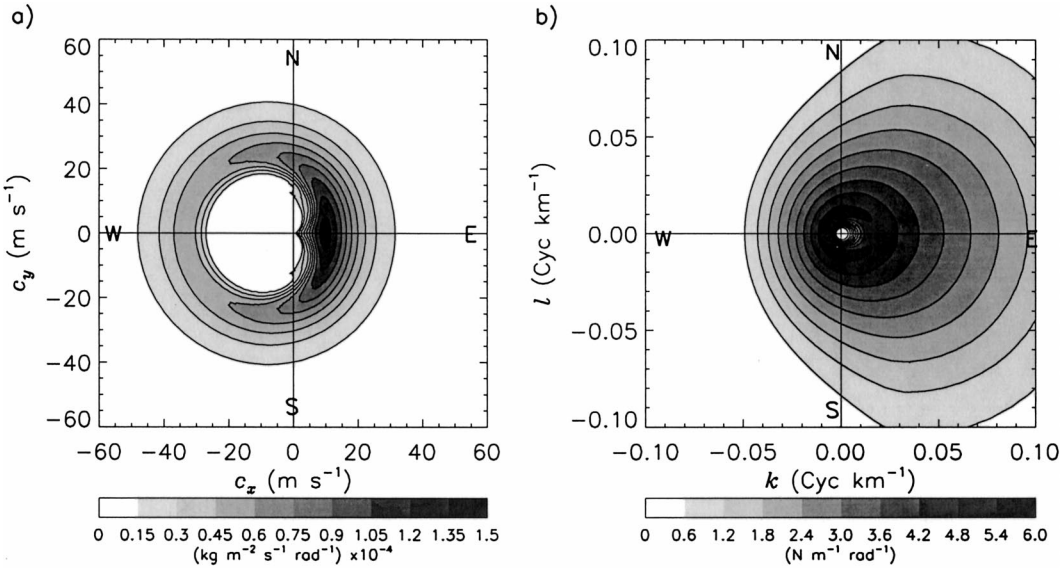

FIG. 4. Same as in Fig. 3 but for $\overline{U} = -10$ m s^{-1} ($\overline{V} = 0$).

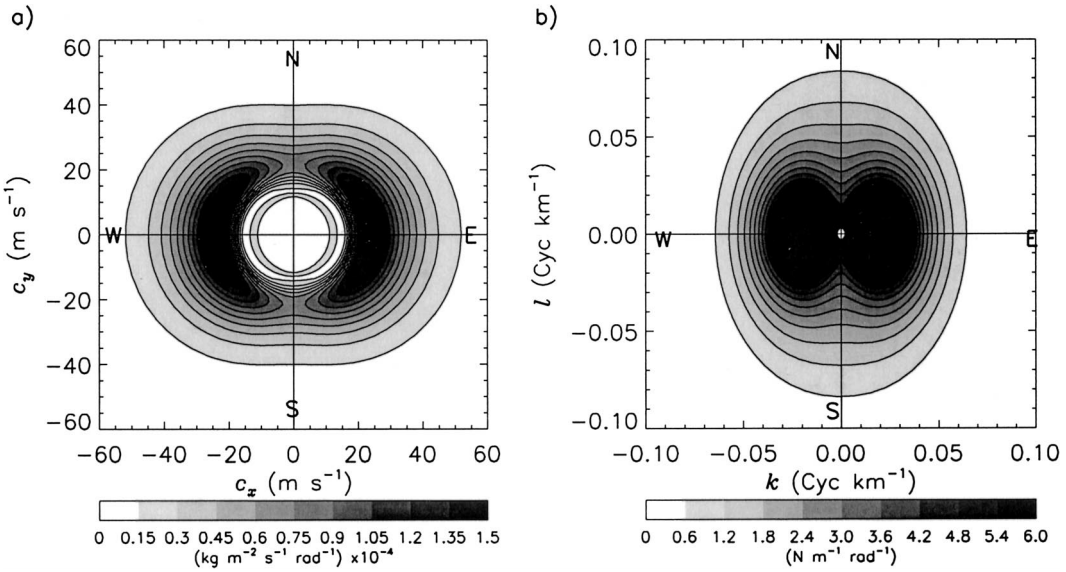

FIG. 5. Same as in Fig. 3 but for $\sigma_x = 6$ km and $\sigma_y = 3$ km.

as the depth of the heating region increases. With increasing heating depth, the width of the momentum flux phase speed spectrum increases, while the momentum flux integrated over all phase speeds stays almost constant with changing *h.* In short, for the same heating rate and horizontal scale, shallow convection produces narrow spectra (in phase speed) with larger peak momentum flux values, while a deep forcing produces a broad spectrum with relatively smaller peak momentum flux values.

The horizontal scale of convection mainly influences the total momentum flux magnitude in a given direction carried by gravity waves. For typical tropical convective heating depth of $h \sim 10$ km, the total momentum flux approximately doubles as the horizontal scale doubles (Fig. 2d). For σ_x values typical for convective cells, between 2 and 10 km, changes in h alter the total momentum flux, however, these changes are much smaller than those due to variations in σ_x.

Figure 2 has important implications for parameterizing gravity waves: In the stratosphere, gravity waves primarily break due to critical-level filtering. Since the phase speed of thermally forced waves for typical convective-sized cells depends primarily on the heating depth, its estimation is crucial to determining wave breaking levels in the stratosphere. The force on the mean flow is proportional to the momentum flux amplitude carried by gravity waves, therefore stratospheric wave forcing is also dependent on the horizontal scale of convection. Gravity waves in the mesosphere and thermosphere break primarily due to unstable amplitudes; in this case the breaking level is dependent on the wave amplitude and horizontal wavelength. Therefore, proper assumptions about the horizontal scale of the heating are crucial to proper representation of gravity wave forcing the mesosphere.

c. Effects of mean wind

Beres et al. (2002) and Beres et al. (2004) noted that tropospheric wind shear alters the symmetry of a convectively forced gravity wave spectrum. Next we show how a unidirectional mean wind within the heating region changes wave propagation in all azimuthal directions. We consider a heating region with the same parameters as the heating used in section 3a and we look at momentum flux for waves with periods between 10 and 100 min.

Figure 3 shows a polar contour plots of $F_{\phi\overline{c}}$ and $F_{\phi\overline{k}}$ for $\overline{U} = \overline{V} = 0$. As expected, wave momentum flux is distributed equally in all directions with dominant phase speed in all directions of 21 m s^{-1} and dominant horizontal wavenumber of 0.01 cpk. For comparison, Fig. 4 shows the same information but for thermally forced waves in the presence of a -10 m s^{-1} zonal mean wind ($\overline{U} = -10$ m s^{-1}, $V = 0$). As stated in (50), the mean wind impacts most wave propagation in the direction of and opposite to the mean wind. Compared to the case of $\overline{U} = 0$, eastward momentum flux carried by gravity waves increases strongly and the westward momentum flux decreases. The distribution of momentum flux across horizontal wavenumbers for eastward-propagating waves is broader than in the zero mean wind case and the opposite is true for westward-propagating waves.

As the angle away from the mean wind increases, and the projection of the mean wind onto the wave direction decreases, so do the effects of the mean wind on wave generation. As ϕ approaches $\pi/2$ and $3\pi/2$, the projection of $\overline{U}$ goes to 0 and the wave spectrum resembles that in no-mean wind conditions.

d. Effects of asymmetry of the heating

In the previous sections we have assumed that convective cells have the same width in all azimuthal directions. Although in a globally averaged sense, this is likely to be a correct assumption, locally convective complexes are sometimes oval shaped. Numerical convection simulations by both Lane et al. (2001) and Piani and Durran (2001) showed convective complexes that were elongated, with the diameter in the longer direction up to 5 times larger than in the shorter direction. Figure 5 shows the distribution of momentum flux generated by a thermal forcing with $\sigma_x = 6$ km and $\sigma_y = 3$ km. Since for a given heating depth, wave momentum flux is almost directly proportional to $\tilde{\sigma}_{xy}$ [see (23) and (12)], wave momentum flux carried by gravity waves in the eastward and westward directions is twice as large as that in the north and south directions. As the wave propagation angle approaches the north or the south direction, the effective horizontal heating scale decreases and the wave spectra converge toward that shown in Fig. 3. For a cell with $\sigma_x = 5\sigma_y$ (typical of convection as noted earlier), momentum flux amplitudes would be 5 times as large in the zonal direction compared to the meridional direction. An asymmetric heating source also causes the horizontal wavelength of generated gravity waves to be different in all directions as shown in Fig. 5b.

4. Summary and conclusions

Convectively generated gravity waves are in part thermally forced. Linear theory with the assumption that gravity waves are solely thermally forced is a good proxy for estimating the spectral properties of convectively forced gravity waves (Beres et al. 2004; Song et al. 2003). Observational and numerical studies of convectively forced waves have noted that gravity waves are generated in three dimensions; this is true even for squall line convection, since a substantial portion of the wave generation occurs in small convective cells with diameters of only several kilometers (e.g., Piani and Durran 2001).

In this work we have presented linear analysis of three-dimensional thermally forced gravity waves and presented equations for specifying wave momentum flux at the top of the forcing region based on the heating properties. We have shown that a three-dimensional wave forcing problem can be treated as a multiple two-dimensional problem by the means of a squire transformation. In other words we have shown that the gravity wave spectrum in a given azimuthal direction depends on the heating and mean wind projection in that direction. We have quantified the relationships between the horizontal and vertical scales of convection and horizontal and vertical wavelength of gravity waves (Fig. 2) and have shown that the vertical scale of the heating has the dominant influence on both the horizontal and vertical wavelength of convectively generated gravity waves. The horizontal scale of the heating, however, strongly influences the wave amplitudes.

As Horinouchi et al. (2002) speculated, both small convective cells with horizontal scale of 1–4 km and aggregates of smaller cells (mesoscale convective systems) can contribute to wave generation. Asymmetric convective cells contribute to creating an anisotropic wave field above the source region, both in the amplitude and spectral characteristics of the gravity waves.

In this study we have also shown how mean wind within the heating region creates an anisotropy in a three-dimensional gravity wave field. For a frequency distribution of heating representative of convection, mean wind in the heating region reduces the wave response in the direction of the mean wind and enhances the response mostly in the direction opposite the mean wind (Fig. 4). These changes compared to a no-mean wind atmosphere decrease as the angle away from the mean wind increases (zero effect for waves perpendicular to the mean wind vector).

Our study suggests that in order to globally parameterize convectively generated gravity waves, information is necessary on the size and frequency distribution of convective cells within a region the size of a GCM grid box. This information is currently not available in GCMs. Such information can, however, be deduced from numerical simulations of convection and it is available from the Global Atmospheric Research Program Atlantic Tropical Experiment (GATE) observational campaign. A new convective parameterization scheme implemented in GCMs, such as one by Donner (1993) with more details about convection characteristics would greatly aid the linking of a gravity wave parameterization to a convection scheme in GCMs.

REFERENCES

Alexander, M. J., and R. A. Vincent, 2000: Gravity waves in the tropical lower stratosphere: A model study of seasonal and interannual variability. *J. Geophys. Res.,* **105** (D14), 17 983–17 993.

——, J. R. Holton, and D. R. Durran, 1995: The gravity wave response above deep convection in a squall line simulation. *J. Atmos. Sci.,* **52,** 2212–2226.

Beres, J. H., M. J. Alexander, and J. R. Holton, 2002: Effects of tropospheric wind shear on the spectrum of convectively generated gravity waves. *J. Atmos. Sci.,* **59,** 1805–1824.

——, ——, and ——, 2004: A method of specifying the gravity wave spectrum above convection based on latent heating properties and background wind. *J. Atmos. Sci.,* **61,** 324–337.

Boville, B. A., 1995: Middle atmosphere version of CCM2 (MACCM2): Annual cycle and interannual variability. *J. Geophys. Res.,* **100** (D5), 9017–9039.

Clark, T. L., T. Hauf, and J. P. Kuettner, 1986: Convectively forced internal gravity waves: Results from two-dimensional numerical experiments. *Quart. J. Roy. Meteor. Soc.,* **112,** 899–925.

Dewan, E. M., and Coauthors, 1998: MSX satellite observations of thunderstorm-generated gravity waves in mid-wave infrared images of the upper stratosphere. *Geophys. Res. Lett.,* **25,** 939–942.

Donner, L. J., 1993: A cumulus parameterization including mass fluxes, vertical momentum dynamics, and mesoscale effects. *J. Atmos. Sci.,* **50,** 899–906.

Dunkerton, T. J., 1997: The role of gravity waves in the quasi-biennial oscillation. *J. Geophys. Res.*, **102** (D22), 26 053–26 076.

Fovell, R., D. Durran, and J. R. Holton, 1992: Numerical simulations of convectively generated stratospheric waves. *J. Atmos. Sci.*, **49,** 1427–1442.

Fritts, D., and M. J. Alexander, 2003: Gravity wave dynamics and effects in the middle atmosphere. *Rev. Geophys.*, **41,** 1003, doi: 10.1029/2001RG000106.

Gage, K. S., and W. H. Reid, 1968: The stability of thermally stratified plane Poiseuille flow. *J. Fluid Mech.*, **50,** 21–32.

Holton, J. R., J. H. Beres, and X. Zhou, 2002: On the vertical scale of gravity waves excited by localized thermal forcing. *J. Atmos. Sci.*, **59,** 2019–2023.

Horinouchi, T., T. Nakamura, and J. Kosaka, 2002: Convectively generated mesoscale gravity waves simulated throughout the middle atmosphere. *Geophys. Res. Lett.*, **29,** 2007, doi:10.1029/2002GL016069.

Kim, Y., S. D. Eckermann, and H. Chun, 2003: An overview of the past, present and future of gravity-wave drag parameterization for numerical climate and weather prediction models. *Atmos.–Ocean*, **41,** 65–98.

Lane, T. P., M. J. Reeder, and T. L. Clark, 2001: Numerical modeling of gravity wave generation by deep tropical convection. *J. Atmos. Sci.*, **58,** 1249–1274.

Lindzen, R. S., 1981: Turbulence and stress owing to gravity wave and tidal breakdown. *J. Geophys. Res.*, **86** (C10), 9707–9714.

Pandya, R. E., and M. J. Alexander, 1999: Linear stratospheric gravity waves above convective thermal forcing. *J. Atmos. Sci.*, **56,** 2434–2446.

Piani, C., and D. Durran, 2001: A numerical study of stratospheric gravity waves triggered by squall lines observed during the TOGA COARE and COPT-81 experiments. *J. Atmos. Sci.*, **58,** 3702–3723.

Song, I.-S., H.-Y. Chun, and T. P. Lane, 2003: Generation mechanisms of convectively forced internal gravity waves and their propagation to the stratosphere. *J. Atmos. Sci.*, **60,** 1960–1980.